# Nanoscale

Accepted Manuscript


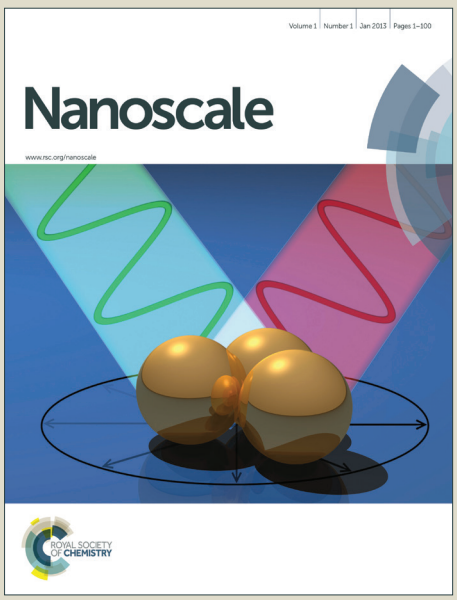





ROYAL SOCIETY OF CHEMISTRY

www.rsc.org/nanoscale

# Ultra-sensitive flow measurement in individual nanopores through pressure - driven particle translocation†

**Alessandro Gadaleta,[a] Anne-Laure Biance,[a] Alessandro Siria,[*,b] and Lyderic Bocquet[b]**

[a] ILM, Université Lyon 1 and CNRS, UMR 5306, 69622 Villeurbanne, France;
[b] Laboratoire de Physique Statistique, E´cole Normale Supe´rieure and CNRS, UMR 8550, 75231 Paris, France.
[*] e-mail: alessandro.siria@lps.ens.fr

A challenge for the development of nanofluidics is to develop new instrumentation tools, able to probe the extremely small mass transport across individual nanochannels. Such tools are a prerequisite for the fundamental exploration of the breakdown of continuum transport in nanometric confinement. In this letter, we propose a novel method for the measurement of the hydrodynamic permeability of nanometric pores, by diverting the classical technique of Coulter counting to characterize a pressure-driven flow across an individual nanopore. Both the analysis of the translocation rate, as well as the detailed statistics of the dwell time of nanoparticles flowing across a single nanopore, allow us to evaluate the permeability of the system. We reach a sensitivity for the water flow down to a few femtoliters per second, which is more than two orders of magnitude better than state-of-the-art alternative methods.

## Introduction

The study of nanoscale liquid flows, commonly coined nanofluidics, has seen a strong increase in attention in the last few years [1-3] . Several new areas of interest have emerged, involving molecular nanopore sensing [4-7] , complex electrochemical effects [8, 9] , as well as permeability enhancement in carbon nanotubes [10, 11] and aquaporins [12] . On the one hand, the discovery of surprising transport phenomena in both biological and artificial systems suggests the possibility of engineering nanostructures to obtain technologicaly useful effects: filtration, desalination, generation of power from osmotic gradients [13]. On the other hand, nanometric sized channels and pores are already exploited and investigated as probes for molecular sensing, especially due to the possibility to achieve low-cost, high-throughput DNA sequencing [14, 15]. New developments open the possibility of using engineered nanopores to significantly improve the sequencing performance, for example by slowing down DNA translocation [16] . Techniques for detection and analysis of single particles or molecules are increasingly popular [17] , applied not only to nucleic acids but also to proteins [18, 19] , polymers [20, 21] and colloidal particles [22] . All of these rely on the resistive-pulse method, pionereed by W. H. Coulter in 1953 [23] and still used in some cytometry applications. The basic idea of the Coulter counter is simple and effective: the analytes, suspended in an electrolyte, are driven by a forcing gradient through a pore of appropriate size. Passage across the pore is detected through the increase in electrical resistance of the system, caused by the displacement of a part of the electrolyte from the internal volume of the pore by the translocating analyte. Shape, intensity and frequency of the resistance pulses allow to infer size, charge and concentration of the particles when the properties of the pore are well known.

A central, unsolved problem of nanofluidics is the measurement of fluid flow and, consequently, of hydraulic permeability of *individual* nanoscale channels. Flows in these systems are often of the order of a few $\mathrm{pL\,s^{-1}}$ or less, two or three orders of magnitude less than the sensitivity of the best commercial flow measurement devices‡. The existing measurement techniques at such small flow rates rely on a technological access to the nanochannel, e.g. electrode grafting [24] or via optical techniques [25] . A smart, alternative method was proposed recently by Keyser et al. [26] , which makes use of truncated colloids as a local probe for the vorticity field outside of the pore, from which the flow rate can be extracted. Typically these methods now allow to measure very small flow rates down to tens of picoliters per second.

However a strong increase in sensitivity is still required to measure flow rates out of nanometric systems, such as nanopores drilled in solid state membranes or graphene, or carbon nanotubes. For example, the flow rate across a nanotube with radius 5 nm, length 1 µm, under a pressure drop of 1 bar is expected to be $Q \approx 2 \cdot 10^{-2}$ $\mathrm{fL\,s^{-1}}$ with no-slip boundary conditions on its surface, while a surface slip length of 100 nm would increase the flow rate up to $Q \approx 2$ $\mathrm{fL\,s^{-1}}$ There is accordingly a crucial need to develop a technique capable of measuring such minute flow rates. In particular such a measurement would dispel any remaining doubts on the ultra-fast water transport in CNTs [10] , associated with large slip lengths on their surface, and would allow to better characterize the properties of biological pores like aquaporins [12, 27] .

In this work, we propose to reverse the standard paradigm of the Coulter counter technique, and use a known colloidal suspension as a probe to measure an unknown pressure-driven flow in a nanometric pore with high sensitivity and accuracy.

Specifically, we demonstrate the feasibility of this method by measuring a flow rate down to about $10^{-14}$ $Ls^{-1}$ with a sensitivity of the order of a $fL\,s^{-1}$ in a low-aspect ratio solid-state nanopore, nanometric in every dimension.

## Results and discussion

Nanopores with diameters around 150–200 nm were fabricated by focused ion beam (FIB) milling in commercial silicon nitride membranes, 50 nm thick. The membranes were mounted in a custom-made fluidic cell[8, 28], separating two electrically isolated reservoirs containing a 1 M KCl solution, buffered at pH 8.3. Ag/AgCl electrodes inside the reservoir were connected to an external patch-clamp amplifier for the electrical measurements. After preliminary measurements, the *cis* reservoir (grounded) was filled with a solution containing 120 nm latex nanoparticles, suspended at a concentration of $10^{11}$ particles/mL, and finally it was connected to an external microfluidic pressure source. The current was measured applying a 10 mV test voltage, while at the same time applying pressure. Events were detected in the current recording using the Open Nanopore Matlab package[29].

Figure **1**(a) depicts 5 s segments of typical current traces, showing clear current pulses caused by particle translocation under pressure drop. The translocation (and thus the flow) is mostly driven by the applied pressure: turning off the pressure gradient, a minority of blockage events remain, which are absent reversing the test voltage. This is consistent with a small electrophoretic flow of the negatively charged colloidal particles, superimposed to the pressure-driven flow. Increasing the applied pressure, the event rate quickly increases, even though the apparent blockade magnitude is smaller.

The experiment was repeated several times, the number of events recorded depending on the lifetime of the pore. In the following, we will show the results of the best experimental run, which recorded about 35k translocation events. Figure **1**(b) shows typical shapes of the current trace during a pressure-driven translocation event, where a triangular shape is observed in good agreement with pulse shapes shown recently in the literature[30, 31] and with most recent numerical calculations[32].

This triangular shape is not due to filtering as the transition width is longer than the 10 $\mu$s filter rise time of the patch-clamp amplifier. Indeed, the combined effect of the spherical shape of the particle and the low aspect ratio of the nanopore, in which entrance effects are important as discussed in the following, results in a non-square current blockade as the resistance continuously increases when the particle approaches the pore. The typical signal is superimposed with the box fitting function automatically created by the Open Nanopore software. While the box fit has a shape considerably different from the current pulse, it still correctly identifies its depth and its length.

Events start and end points are actually identified as the points where the signal differs from the local baseline more than a threshold set by the local standard deviation[29], disentangling their determination from the fitting procedure. While all analyzed events are longer than the filter rise time, the shape of the current pulse can be influenced by the filtering in its steepest part, i.e. the bottom, rendering the determination of the pulse depth unreliable. Event start and end times were collected by the software for each current recording, allowing to investigate the basic event statistics. Figure **2**(a) shows an histogram of the time interval between each event, for a current recording taken at 10 mbar applied pressure. The histogram can be accurately fitted by an exponential distribution function:

$$n(\Delta t) \propto e^{-\Delta t/\langle \Delta t \rangle} \quad (1)$$

with $n$ being the frequency of an interval of length $\Delta t$, showing that the translocation events are a memory-less Poisson process at the colloid concentration used.

From the exponential fit, a characteristic time $\langle \Delta t \rangle$ and a translocation rate, calculated as $f = 1/\langle \Delta t \rangle$, can be extracted for each experiment. Similarly, we can extract and plot the event dwell times for the same recording, as shown in figure **??**(b). In this case, the distributions can be fitted by a inverse Gaussian law:

$$n(\tau) \propto \sqrt{\frac{\lambda}{2\pi\tau^3}}\, exp\left\{\frac{-\lambda(\tau-\langle\tau\rangle)}{2\tau\langle\tau\rangle^2}\right\} \quad (2)$$

where $\tau$ is the average dwell time and $\lambda$ is the shape parameter. This distribution is well known to describe the time of first passage in a Brownian motion with added drift[33]. In our case, the effect of Brownian motion is expected to be small in comparison with the external pressure-driven flow. Nevertheless, this function and others asymmetrical variations of the normal distribution have been shown[31] to phenomenologically provide a good fit of translocation dwell time distributions. Other possible phenomena underlying the shape of this distribution could be related to tha particle size distribution[31] and the starting position of the particles[30]. From this fit, the most probable value of the dwell time can be calculated as the mode of the distribution:

$$\tau^* = \tau\left[\sqrt{1+\left(\frac{3\tau}{2\lambda}\right)^2} - \frac{3\tau}{2\lambda}\right] \quad (3)$$

These statistical analyses are performed for different applied pressure between the reservoirs. Figure **3** shows a plot of the translocation rate $f$ on the same 171 nm nanopore, for different applied pressures. Excluding the point at highest pressure, a linear dependence of the rate on the pressure is recovered. The deviation from linearity at larger pressure can be attributed to the fact that the dwell time distribution starts to dip into the zone near and under the 10 µs filter rise time, pushing a non negligible part of the events under the noise threshold, and causing an error in the rate estimation. The raw data (shown in the inset) present

a non-zero intercept, due to electro-phoretic and electro-osmotic contributions to the flow. In order to explore only the effect of the pressure-driven flow, this constant contribution has been removed in the main diagram.

The linearity of the event frequency with the forcing gradient has already been verified both for electrophoresis[31] and pressure-driven translocation [34, 35], but no accurate measurements of permeability have been proposed. This behavior can be easily modeled. Assuming laminar (Stokes) flow, a particle is an accurate tracer of the flow if the Stokes number[36] $\mathrm{St} = \rho d^2/18\eta t$ (with $C$ density, $d_c$ colloidal particle diameter, $\eta$ fluid viscosity and $t$ a characteristic time such as the dwell time) is much smaller than unity, which is the case here ($\mathrm{St} \approx 0.1\%$). In absence of gravitational effects, the volume occupied by such a tracer in a pressure-driven flow is equivalent to any fluid volume, and then the translocation frequency is given by

$$f = QC \quad (4)$$

with $C$ the nanoparticle concentration and $Q$ the hydrodynamic flow through the nanopore. The non-zero intercept in the inset of figure **3** has to be interpreted as residual translocation events driven by electrophoresis. Equation **4** clearly allows to directly infer the flow from a measurement of the translocation rate. From the linear fit in figure **3**, we can estimate the hydrodynamic permeability of the nanopore as $(13.2 \pm 0.3)$ fL s$^{-1}$ mbar$^{-1}$. This value can be compared to theoretical predictions, assuming a Hagen-Poiseuille flow inside the pore and Sampson flow[37, 38] at the pore entrances, giving:

$$Q = \frac{\Delta P}{\eta}\left(\frac{3}{r^3} + \frac{8l}{\pi r^4}\right)^{-1} \quad (5)$$

with $r$ the pore radius and $l$ the pore length, yielding a permeability of 13.9 fL s$^{-1}$ mbar$^{-1}$. This is in good agreement with experimental results. We attribute the small discrepancy to systematic errors in the colloid concentration. Let us note this is the first time that such a flow rate has been quantitatively measured with this technique.

This technique relies on the value of the particle concentration, which is not always possible to evaluate, for example when colloid exclusion is achieved near charged surfaces. It assumes also that no interaction energy has to be overcome during the translocation, which is not the case in many molecular systems[39] . Disentangling flow rate measurement from probe concentration would be a great advance for permeability determination in more complex systems. Investigation of the pressure dependence of the dwell time should therefore be a method of choice for permeability measurements.

Figure **4**(a) shows a plot of the dwell time $\tau^*$, for different applied pressures, while figure **4**(b) shows a plot of its inverse $1/\tau^*$, proportional to the translocation velocity of the nanoparticles, corrected for the zero-pressure intercept. Unlike the translocation rate data in figure **3**, the linear fit is satisfactory up to all applied pressure, showing that the loss of the shorter events due to filtering does not significantly affect the distribution fit in our experimental conditions. The permeability estimation from dwell time measurements is then expected to be more reliable in most experimental conditions.

However, in order to link the measured dwell time to the particle velocity and to the flow rate, one has to consider the length on which the particle is detected electrically. In a low aspect ratio nanopore, the access resistance has an important role in determining the shape of the resistive pulse. The translocation event can be detected in the current trace earlier than the entrance of the particle inside the pore[32, 40], so that the effective translocation length is longer than the pore length. It depends on pore geometry and measurement noise. In a high-aspect ratio pore, instead, the effect of the access resistance becomes negligible[40, 41] and the translocation length can be assumed to be equal to the pore length, which is often known or measurable. In the general case of a low-aspect ratio pore, maybe of unknown or complicated geometry, it may be necessary to resort to detailed numerical calculations[32] in order to obtain a theoretical current vs. time curve to compare with experimental current pulses. As these calculations are outside the scope of this work, we limit ourselves to a simple order-of-magnitude estimate of the actual detection length $l_d$. Let us consider that an event is detected when the current pulse emerges from the noise ($\Delta I > 5I_{\mathrm{RMS}}$). Current blockage ratio $i = \Delta I/I$ is known to be[31] roughly proportional to the volume of the colloid divided by the volume of interest. Considering entrance effects and neglecting pore surface charge at this salt concentration[28], the volume of interest is equal to the pore volume plus an entrance hemisphere having a radius $z_d$, with $z_d$ detection distance as shown in figure **??**(c). If $d_c$ is the colloid diameter, a colloid will be detected at a distance given by:

$$i = \frac{\pi d_c^3/6}{\pi d^2 l + 4\pi d z_d^2/3} \quad (6)$$

In our experimental conditions ($i \approx 0.04$ at the detection threshold) we get $l_d = 2z_d + l \approx 370$ nm. Typical translocation velocities, calculated using this value of detection length, are of the order of 2 mm/s for a 10 mbar applied pressure. At a distance $z \gg l$ from the pore, we can also approximate $v(z) \approx Q/2\pi z^2$. Integrating over the detection length, we get for a formula for the flow rate:

$$Q \approx \frac{4\pi z_d^3}{3\tau^*} + \frac{\pi l d^2}{4\tau^*} \quad (7)$$

Comparing with the linear fit in figure **4**(b), we estimate the flow rate to be approximately 11.3 fL s$^{-1}$ mbar$^{-1}$, which, given the rough approximations involved, can be considered in good agreement with value estimated from the translocation rate. In principle, the detection length could be estimated by comparing results obtained with different pore sizes. In practice, however, when using nanometric pores the commercial selection of nanoparticle sizes is limited, and the choice of size is dictated by sensitivity and pore lifetime considerations. These two measurements allow the determine the permeability of the pores with a

huge sensitivity. In both cases, the main technical limitation relies on event detection, which is set by filter rise time and noise level. In the case of frequency determination, one can assume events will be missed if the translocation time is smaller than the filter rise time (10 $\mu$s). This filter rise time sets also an error bar on dwell time determination. Let's mention that electrokinetic effects such as streaming current induced by charged pores or colloid electrophoresis can have dramatic effects on dwell time absolute value, putting it under the sensitivity limit.

and are then useful to slow down colloids if applied in the good direction.

Beyond his technical limitation, these two measurements have intrinsically different advantages and limitations. Concerning the frequency measurement, the measurement relies on a knowledge of local colloid concentration. If depletion or enrichment of colloids is observed at the pore entrance or inside the pore, this measurement could lead to improper determination of the permeability. This will be the case if the pore acts as partially selective membrane for the colloids, for example in the case of Debye layer overlap within the system[2]. In the case of dwell time analysis, the colloid local concentration is not so crucial. However, permeability evaluation relies on the determination of a detection length, which will depend on the geometry of the system (in the present case of nanopore, the aspect ratio is for example to be known). Note that for more common geometries where access resistance is negligible (nanotube for example), system size is not a requirement for flow rate estimation and the only limitation in this case will be technical.

## Conclusions

In conclusion, we demonstrated that a pressure-driven flow through a nanopore can be measured with good accuracy through a simple Coulter counting of nanoparticles, driven to translocate across the pore by the pressure gradient. While the flow measurement itself only relies on the translocation rate, the information gathered from the particle dwell times could be used to further characterize the studied nanostructure. To the best of our knowledge, this is the first accurate measurement of Pouseuille flow in a nanometric pore or channel, which does not rely on an optical technique or nano-electrode grafting. We are able for the first time to measure flow rates of typically $\approx 20$ fL s$^{-1}$, with a sensitivity down to about a fL s$^{-1}$. While we used latex nanoparticles, this experiment could be reproduced in this and other systems using different colloidal probes, like polymers or nucleic acids, as long as their interaction with the pore surface is well characterized. We are confident that the method we presented will allow to shed some light on the properties of the pore/fluid interface in interesting systems like nanotubes or biological pores.

## Acknowledgments

We thank R. Fulcrand for nanopore FIB milling and S. Gravelle and C. Sempere for useful discussions. We acknowledge financial support from the ERC-AG project *Micromegas* and the ANR project *Blue Energy*.

## References

1 J. C. Eijkel and A. Van Den Berg, Microfluid. and Nanofluid., 2005, 1, 249–267.

2 L. Bocquet and E. Charlaix, Chem. Soc. Rev., 2010, 39, 1073–95.

3 L. Bocquet and P. Tabeling, Lab Chip, 2014, 14, 3143–3158.

4 H. Bayley and C. R. Martin, Chem. Rev., 2000, 100, 2575–2594.

5 C. Dekker, Nat. Nanotechnol., 2007, 2, 209–2015.

6 B. N. Miles, A. P. Ivanov, K. A. Wilson, F. Dogan, D. Japrung and J. B.Edel, Chem. Soc. Rev., 2013, 42, 15–28.

7 U. F. Keyser, J. R. Soc., Interface, 2011, 8, 1369–1378.

8 A. Siria, P. Poncharal, A.-L. Biance, R. Fulcrand, X. Blase, S. T. Purcell and L. Bocquet, Nature, 2013, 494, 455–458.

9 C. B. Picallo, S. Gravelle, L. Joly, E. Charlaix and L. Bocquet, Phys. Rev. Lett., 2013, 111, 244501.

10 J. K. Holt, H. G. Park, Y. Wang, M. Stadermann, A. B. Artyukhin, C. P. Grigoropoulos, A. Noy and O. Bakajin, Science,

2006, 312, 1034–1037.

11 K. Falk, F. Sedlmeier, L. Joly, R. R. Netz and L. Bocquet, Nano Lett., 2010, 10, 4067–4073.

12 K. Murata, K. Mitsuoka, T. Hirai, T.Walz, P. Agre, J. B. Heymann, A. Engel and Y. Fujiyoshi, Nature, 2000, 407, 599–605.

13 B. E. Logan and M. Elimelech, Nature, 2012, 488, 313–319.

14 D. Branton, D. W. Deamer, A. Marziali, H. Bayley, S. A. Benner, T. Butler, M. Di Ventra, S. Garaj, A. Hibbs and X. Huang, Nature, 2008, 26, 1146–1153.

15 B. M. Venkatesan and R. Bashir, Nature Nanotechnol., 2011, 6, 615–624.

16 T. Z. Butler, M. Pavlenok, I. M. Derrington, M. Niederweis and J. H.Gundlach, Proc. Natl. Acad. Sci., 2008, 105, 20647–20652.

17 R. R. Henriquez, T. Ito, L. Sun and R. M. Crooks, Analyst, 2004, 129, 478–482.

18 G. Oukhaled, J. Mathe, A.-L. Biance, L. Bacri, J.-M. Betton, D. Lairez, J. Pelta and L. Auvray, Phys. Rev. Lett., 2007, 98, 158101.

19 C. Plesa, S. W. Kowalczyk, R. Zinsmeester, A. Y. Grosberg, Y. Rabin and C. Dekker, Nano Lett., 2013, 13, 658–663.

20 B. Lu, D. P. Hoogerheide, Q. Zhao, H. Zhang, Z. Tang, D. Yu and J. A. Golovchenko, Nano Letters, 2013, 13, 3048–3052.

21 A. G. Oukhaled, A.-L. Biance, J. Pelta, L. Auvray and L. Bacri, Physical Review Letters, 2012, 108, 088104.

22 T. Ito, L. Sun and R. M. Crooks, Anal. Chem., 2003, 75, 2399–2406.

23 W. H. Coulter, Means for counting particles suspended in a fluid, 1953, US Patent 2,656,508.

24 K. Mathwig, D. Mampallil, S. Kang and S. G. Lemay, Phys. Rev. Lett., 2012, 109, 118302.

25 C. Lee, C. Cottin-Bizonne, A.-L. Biance, P. Joseph, L. Bocquet and C. Ybert, Phys. Rev. Lett., 2014, 112, 244501.

26 N. Laohakunakorn, F. Gollnick, B.and Moreno-Herrero, D. G. A. L. Aarts, R. P. A. Dullens, S. Ghosal and U. F. Keyser, Nano Lett., 2013, 13, 5141–5146.

27 S. Gravelle, L. Joly, F. Detcheverry, C. Ybert, C. Cottin-Bizonne and L. Bocquet, Proc. Natl. Acad. Sci., 2013, 110, 16367–16372.

28 C. Lee, L. Joly, A. Siria, A.-L. Biance, R. Fulcrand and L. Bocquet, Nano Lett., 2012, 12, 4037–44.

29 C. Raillon, P. Granjon, M. Graf, L. Steinbock and A. Radenovic, Nanoscale, 2012, 4, 4916–4924.

30 L. J. Stober, G.and Steinbock and U. F. Keyser, J. Appl. Phys., 2009, 105, 084702.

31 M. Davenport, K. Healy, M. Pevarnik, N. Teslich, S. Cabrini, A. P. Morrison, Z. S. Siwy and S. E. L´etant, ACS Nano, 2012, 6, 8366–8380.

32 S. C. Kim, S. K. Kannam, S. Harrer, M. T. Downton, S. Moore and J. M.Wagner, Phys. Rev. E, 2014, 89, 042702.

33 M. C. Tweedie, Ann. Math. Stat., 1957, 362–377.

34 G. Willmott, R. Vogel, S. Yu, L. Groenewegen, G. Roberts, D. Kozak, W. Anderson and M. Trau, J. Phys.: Condens. Matter, 2010, 22, 454116.

35 L. Sun and R. M. Crooks, J. Am. Chem. Soc., 2000, 122, 12340–12345.

36 C. E. Brennen, Fundamentals of multiphase flow, Cambridge University Press, 2005.

37 R. A. Sampson, Philos. Trans. R. Soc., A, 1891, 182, 449–518.

38 R. Roscoe, Philos. Mag., 1949, 40, 338–351.

39 T. Auger, J. Math´e, V. Viasnoff, G. Charron, J.-M. Di Meglio, L. Auvray and F. Montel, Phys. Rev. Lett., 2014, 113, 028302.

40 J. Wang, J. Ma, Z. Ni, L. Zhang and G. Hu, RSC Adv., 2014, 4, 7601–7610.

41 A. Gadaleta, C. Sempere, S. Gravelle, A. Siria, R. Fulcrand, C. Ybert and L. Bocquet, Phys. Fluids, 2014, 26, 012005.

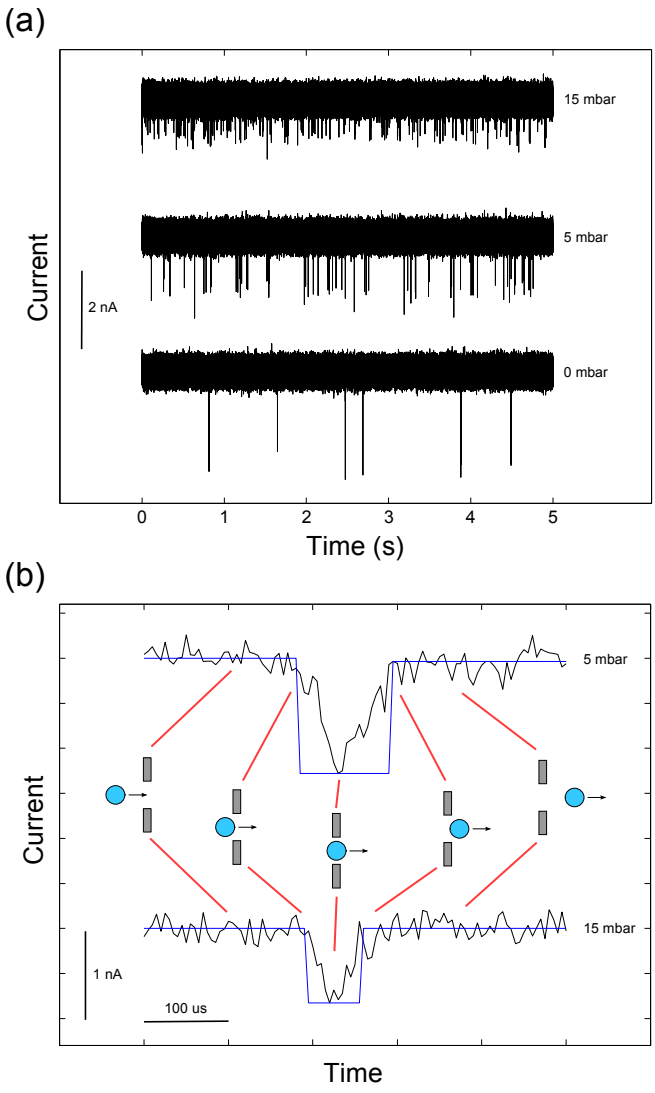


Figure 1 (a) 5 second samples of current traces, recorded with a 10 mV test voltage. The samples show the baseline signal with no applied pressure, and typical signals at 5 and 15 mbar. The average baseline current is about 13.5 nA. (b) Diagram illustarting typical translocation events. The current traces, taken at 5 and 15 mbar applied pressure, are superimposed with the automated box fit produced by the OpenNanopore software.

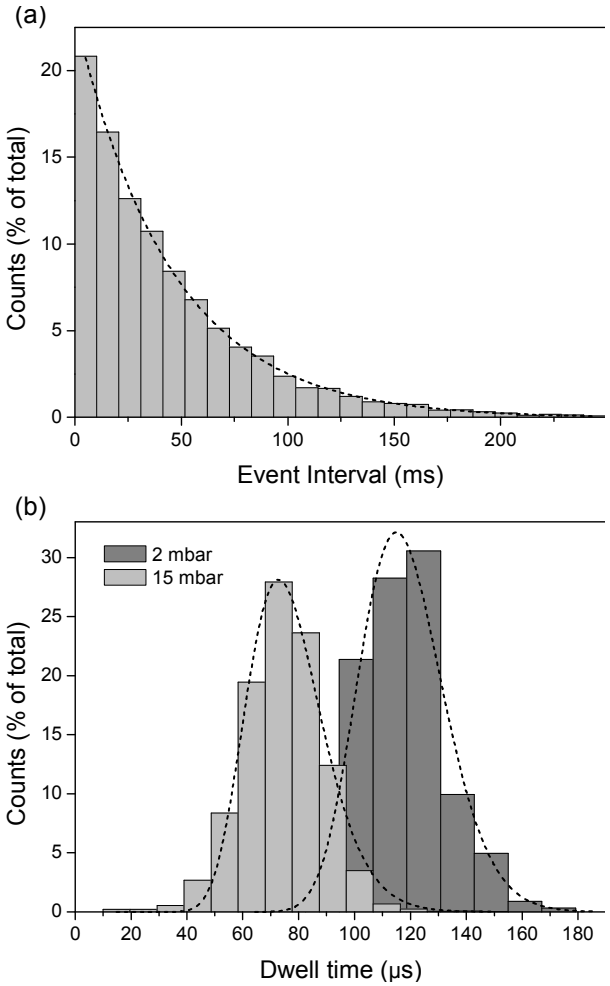


Fig. 2 (a) Normalized histogram of the time interval between successive translocation events, for a 171 nm diameter pore, at 10 mbar applied pressure. Dashed line: exponential fit of the distribution. Event intervals are defined as intervals between the temporal half-point of each event. Given the short duration of the events, alternative definitions give identical results. (b) Normalized histograms of the dwell time (event duration), for the same sample in (a), at 2 mbar (1914 total events) and 15 mbar (9596 total events) applied pressure. Dashed lines: inverse Gaussian fits of the distributions.

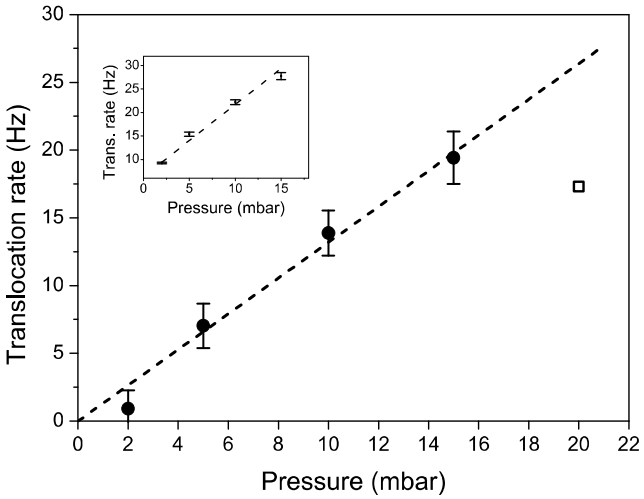

Fig. 3 Inset: translocation rate, estimated from the exponential fit of the interval histogram, for a 171 nm nanopore. The dashed line is a linear fit. Main diagram: translocation rate data, after subtraction of the fit intercept to correct for the electro-phoretic and –osmotic contributions, retaining only the pressure-driven part. The empty square is a "high pressure" data point, showing a large systematic error due to failed detection of a part of the events.

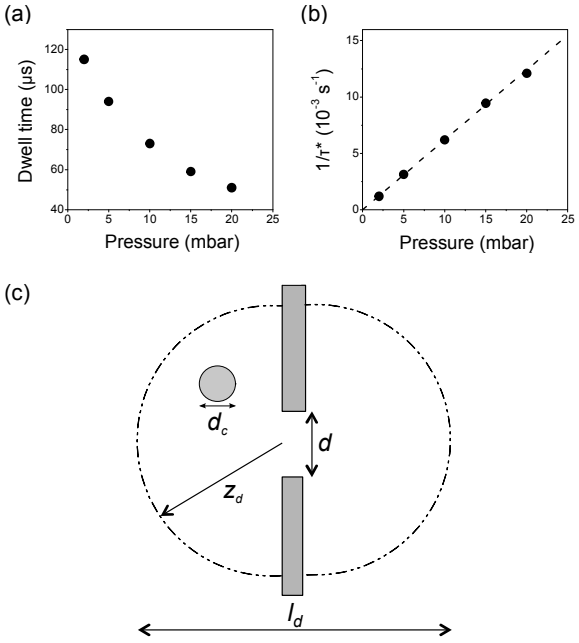


Fig. 4 (a) Most probable value t_ of the dwell time versus applied pressure, calculated from the inverse gaussian fit of the dwell histograms, for a 171 nm nanopore. (b) Inverse of the dwell time 1=t_ versus applied pressure, corrected for the zero-pressure intercept. This value is proportional to the pressure-driven contribution to the translocation velocity of the particles. The dashed line is a linear fit to the data. (c) Diagram of the detection radius zd.